

# Revealing spatio-temporal interaction patterns behind complex cities

Chenxin Liu<sup>1</sup>, Yu Yang<sup>1</sup>, Bingsheng Chen<sup>1,2\*</sup>, Tianyu Cui<sup>1</sup>, Fan Shang<sup>1</sup>, and Ruiqi Li<sup>1\*</sup>

<sup>1</sup>UrbanNet Lab, College of Information Science and Technology, Beijing University of Chemical Technology, Beijing 100029, China

<sup>2</sup>Centre for Complexity Science, Imperial College London, London SW7 2AZ, UK

\*corresponding authors: lir@buct.edu.cn (Ruiqi Li), bingsheng.chen14@imperial.ac.uk (Bingsheng Chen).

## ABSTRACT

Cities are typical dynamic complex systems that connect people and facilitate interactions. Revealing universal collective patterns behind spatio-temporal interactions between residents is crucial for various urban studies, of which we are still lacking a comprehensive understanding. Massive cellphone data enable us to construct interaction networks based on spatio-temporal co-occurrence of individuals. The rank-size distributions of hourly dynamic population of locations are stable, although people are almost constantly moving in cities and hotspots that attract people are changing over time in a day. A larger city is of a stronger heterogeneity as indicated by a larger scaling exponent. After aggregating spatio-temporal interaction networks over consecutive time windows, we reveal a switching behavior of cities between two states. During the “active” state, the whole city is concentrated in fewer larger communities; while in the “sleeping” state, people are scattered in more smaller communities. Above discoveries are universal over diversified cities across continents. In addition, a city sleeps less, when its population grows larger. And spatio-temporal interaction segregation can be well approximated by residential segregation in smaller cities, but not in larger ones. We propose a temporal-population-weighted-opportunity model by integrating time-dependent departure probability to make dynamic predictions on human mobility, which can reasonably well explain observed patterns of spatio-temporal interactions in cities.

## Introduction

The city is a typical complex system that connects people and facilitates interactions between its residents<sup>1,2</sup>. Nonlinear and diversified interactions induced by agglomeration effect with supports from more efficiently utilized infrastructures in cities<sup>3,4</sup> give rise to the increasing return to scale, which can be depicted as a superlinear urban scaling relation between socioeconomic output and urban population<sup>5</sup>. Diverse interactions from different social groups are critical for improving social cohesion<sup>6</sup>, overall safety level<sup>7</sup>, well-beings of residents<sup>8,9</sup>, and the prosperity of the city<sup>10</sup>. Urban geography, social networks, and mobility of residents are crucial for increasing the diversity of interactions<sup>9</sup>. In addition, human interaction activities also exhibit regular patterns<sup>11–13</sup> and strong rhythms that one generally wake up, go to work, back home to rest and eat, or go for entertainments<sup>2</sup>. The city is composed of people and shaped by collective human interactions, we are still lacking a clear picture of interaction patterns at urban scale with a high spatio-temporal resolution. New York, Hong Kong, and Shanghai are among the first a few “sleepless” cities in the world, where interactions are seemingly happening everywhere and every moment. Behind almost non-stop traffic flows, are there any stable and universal patterns of human concentration and interactions in cities? Is a city really sleepless? Is the city center an exceptional aggregator of diversity<sup>14</sup>? Gaining a deeper understanding of spatio-temporal patterns of human interactions in cities is crucial for answering above questions and benefiting various urban studies, including intervening epidemic spreading<sup>15–21</sup>, assisting better urban planning<sup>22</sup>, evaluating segregation<sup>23–26</sup>, traffic engineering<sup>27–30</sup>, resources allocation<sup>31</sup>, emergency management<sup>32,33</sup>.

However, measuring spatio-temporal human interactions at a fine resolution was technically challenging and costly or even impossible at a large scale just a few decades ago<sup>34</sup> until the emergence of massive cellphone data<sup>35</sup>. Mobile phones can be regarded as ubiquitous sensors of various human activities since they are of a very high penetration rate and a lower usage bias across the world<sup>35</sup>. Call and data detailed record (CDDR) of cellphone contains information about both timestamps and locations when anonymized users use the service (e.g., making phone calls, sending texts, or using data by APPs), which is generally of high spatio-temporal resolutions<sup>35</sup>. For example, in some megacities, the spatial resolution of CDDR can be around two hundred meters, and down to tens of meters in the downtown area even around ten years ago<sup>36,37</sup>. After fully upgrading to 4G or 5G networks, the spatio-temporal resolutions of CDDR can be much higher. Therefore, CDDR can be used to infer potential spatio-temporal interactions and mobility patterns of individuals at a fine scale.

In this study, by exploiting massive cellphone data of three diversified cities – Dakar<sup>29</sup>, Abidjan<sup>17</sup>, and Beijing<sup>36,37</sup> – across

continents, we construct interaction networks based on spatio-temporal co-occurrence of individuals to study the emergent collective patterns at the urban scale. Individuals who appeared at the same place at the same time will have a high probability to interact with each other and thus be connected in the spatio-temporal interaction networks. The connection patterns of such networks are dynamic due to human mobility. Though people are almost constantly moving in cities and hotspots that attract people are changing over time in a day, at each snapshot, Zipfian rank-size distributions of hourly dynamic population of locations is stable. After aggregating spatio-temporal interaction networks of two or more consecutive time windows, we observe that cities are switching between “active” and “sleeping” states. During the “active” state, the whole city is largely concentrated in fewer larger communities; while in the “sleeping” state, the whole city is scattered in more smaller communities. The above discoveries are universal over diversified cities across continents. When a city grows larger in terms of population, its sleeping state shortens. For Dakar in Senegal, it sleeps from 0 am to 8 am, Abidjan in Côte d’Ivoire sleeps from 0 am to 6 am, while Beijing only sleeps from 2 am to 6 am. Such discoveries can be informative on assisting urban management. For example, if a city sleeps at 10 pm, then, during a pandemic, setting a curfew from 11 pm will be less effective. In addition, we discover that spatio-temporal interaction segregation can be well approximated by residential segregation in smaller cities, but not in larger cities. We propose a temporal population-weighted opportunity (TPWO) model by incorporating time-dependent departure probability, and it can reasonably well explain observed patterns of spatio-temporal interactions in cities.

## Results

### Data

To construct individual spatio-temporal interaction networks in cities and reveal possible universal patterns behind them, we exploit massive cellphone data of three diversified cities across continents – Dakar<sup>29</sup>, Abidjan<sup>17</sup>, and Beijing<sup>36,37</sup>. These cities are of different urban size, climate, economic development level (see Table 1), and geography (see Supplementary Fig. 1). Beijing, the capital of China, is an international mega city that accommodates more than twenty million people nowadays. Abidjan, the economic center and former capital of Côte d’Ivoire, is one of prosperous cities in Africa. It is also the financial and trade center of West African. Dakar, the capital of Senegal, is relatively underdeveloped.

Call and data detail record (CDDR) of cellphone data contains both location coordinates and timestamps when anonymized customers use the service (e.g., making phone calls, sending texts, or using data by APPs), thus provides rich spatio-temporal information about human mobility patterns. Each CDDR record contains an anonymized user ID, start time, end time, latitude and longitude of the location. The Beijing dataset contains 100,000 subscribers and covers the whole month of December, 2013. After filtering less active users, we end up with 90,500 users. The spatial resolution is quite high for the Beijing dataset indicated by a small median diameter of Voronoi polygons partitioned based on cellphone towers (see Table 1). The Abidjan dataset detailing mobility information of 20,000 users for two weeks<sup>38</sup>. The Dakar dataset covers two weeks for about 120,000 users<sup>39</sup>.

City	Pop.	Area	Temp.	RH	Daylight	GDP p.c.	#Towers	#Users	Resolution	Month
Dakar (Senegal)	2.62 M	202 km <sup>2</sup>	22°C	58%	11.3h	\$ 679	453	59,864	611 m	Jan., 2013
Abidjan (Côte d’Ivoire)	4.06 M	588 km <sup>2</sup>	28°C	84%	11.8h	\$ 1,132	242	12,880	1,185 m	Dec., 2011
Beijing (China)	17.7 M	16,330 km <sup>2</sup>	-9°C	64%	9.5h	\$ 14,745	17,317	90,500	177 m	Dec., 2013

**Table 1.** Basic statistics of cities and cellphone data. RH refers to relative humidity. Area refers to the studied area with coverage by cellphone towers, for Dakar and Abidjan, the area of their administrative region is 544 km<sup>2</sup> and 1,965 km<sup>2</sup>, respectively. Basic statistics of cities are subject to the time period of the dataset. The temperature, humidity, and length of daylight are the average of the month. #Towers refers to the number of cellphone towers in the city related to the dataset. #Users refers to the number of active users used in this study. Resolution refers to the median diameter of Voronoi polygons that are generated based on the spatial distribution of cellphone towers (see Supplementary Fig. 1 and Supplementary Note 1 for more details).

### Constructing spatio-temporal interaction networks

Based on CDDR data, following the framework outlined in<sup>36,37,40,41</sup>, we extract the mobility trajectory of users at high spatio-temporal resolutions (see Supplementary Note 1 for more details). The obtained trajectory tells us when and where the user is, thus individual interaction networks can be inferred based on spatio-temporal co-occurrence. If some users appear at the same place at the same time, then they will be connected in a specific spatio-temporal interaction network (see illustration in Fig. 1). The real spatio-temporal interaction probability between people is affected by the land use type of the location. For simplicity and without losing generality, we make a homogeneous assumption that the chance of interaction between individuals at all locations are the same, which can be suitable for COVID-19 pandemic spreading modeling<sup>20,42</sup>. The highest

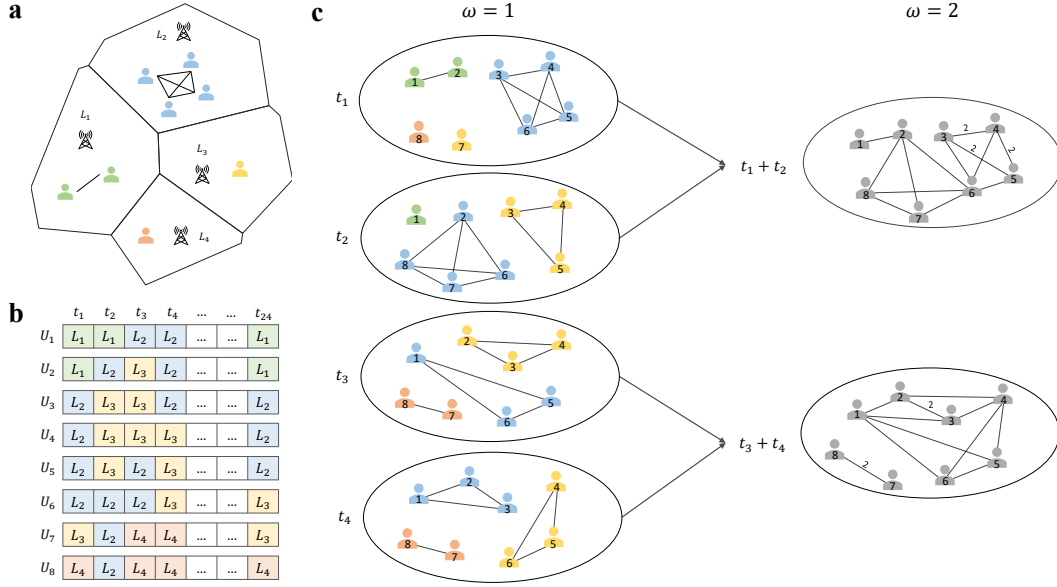


**Figure 1. Schematic diagram of constructing spatial-temporal interaction networks from cellphone data and network aggregation process.** **a** An interaction network is created for each hour based on spatio-temporal co-occurrence. Individuals who appear at the same location at the same  $t$  form a clique, as, for simplicity, we assume the interacting probability is equal to one. **b** The mobility trajectory of individuals. Locations are obtained from Voronoi tessellation based on the spatial distribution of cellphone towers (see Supplementary Fig. 1). In each time window  $t$ , the individual is associated with the location with the longest stay duration (see Supplementary Note 1 for more details). **c** Spatio-temporal interaction networks obtained from **b** at each snapshot (i.e., time window size  $\omega = 1$ ) and the aggregation of spatio-temporal networks over consecutive time windows with  $\omega = 2$ . When aggregating network of snapshots (e.g.,  $t_1$  and  $t_2$ ), links accumulate.

spatial resolution we can obtain is at the location level partitioned according to the spatial distribution of cellphone towers by Voronoi tessellation (see illustration in Fig. 1a and Supplementary Fig. 1). The temporal resolution depends on the frequency of cellphone usage, which can be quite high in the era of 4G and 5G communication. Here, we set it as one hour and associate the location with the longest stay duration to the user in each hour, and the full individual mobility trajectory consists of twenty-four locations (see Fig. 1b).

Due to mobility of individuals (see Fig. 1b), the spatio-temporal network in each time window can be varying (see the left side of Fig. 1c). Aggregating interaction networks over consecutive time windows connects the separated cliques in each snapshot forming more complex structures (see the right side of Fig. 1c). A prominent one is the community structure with more internal connections than external ones, which corresponds to groups of individuals who have more spatio-temporal overlaps with each other. Thus the community structure is a natural way to measure the collective interaction patterns at the urban scale. The mathematical definition of spatio-temporal networks is detailed in Methods.

### The stable rank-size distribution of hourly dynamic population

In a specific spatio-temporal network, the network is composed of disconnected cliques (see Fig. 1a and left side of Fig. 1c), and community detection algorithm returns such divisions (see Fig. 2a). The size of cliques in each location can be interpreted as the dynamic population of that place at that time. To earn their livelihood and meet various needs, people are almost constantly moving in cities<sup>2,44</sup>. Hotspots that attract people evolve over time in a day<sup>45</sup>, for instance, during lunch time, hotspots would move to restaurants, while, during working time, the hotspots might move to CBD and working zones. Thus, it is intriguing that the distribution of hourly dynamic population are fairly stable over time in diversified cities (see Fig. 2a), which might be induced by heterogeneous population distribution and temporal heterogeneity of mobility. Communities are ranked according to their sizes, where the largest one is ranked first and the smallest ranked the last. We find that such Zipfian rank-size distributions of community size of each hour almost collapse together and follow a truncated power-law  $s \propto r(s)^{-\alpha} e^{-r(s)/\kappa}$ , where  $s$  is the community size,  $\alpha$  is the scaling exponent,  $r(s)$  is the rank of the community, and  $\kappa$  is the exponential cut-off (see Supplementary Fig. 2). The scaling exponent  $\alpha$  is larger for cities with more population, which indicates that a larger city has a stronger heterogeneity and diversity that population concentrate in fewer larger communities and the size of communities decays faster (see Supplementary Fig. 2).

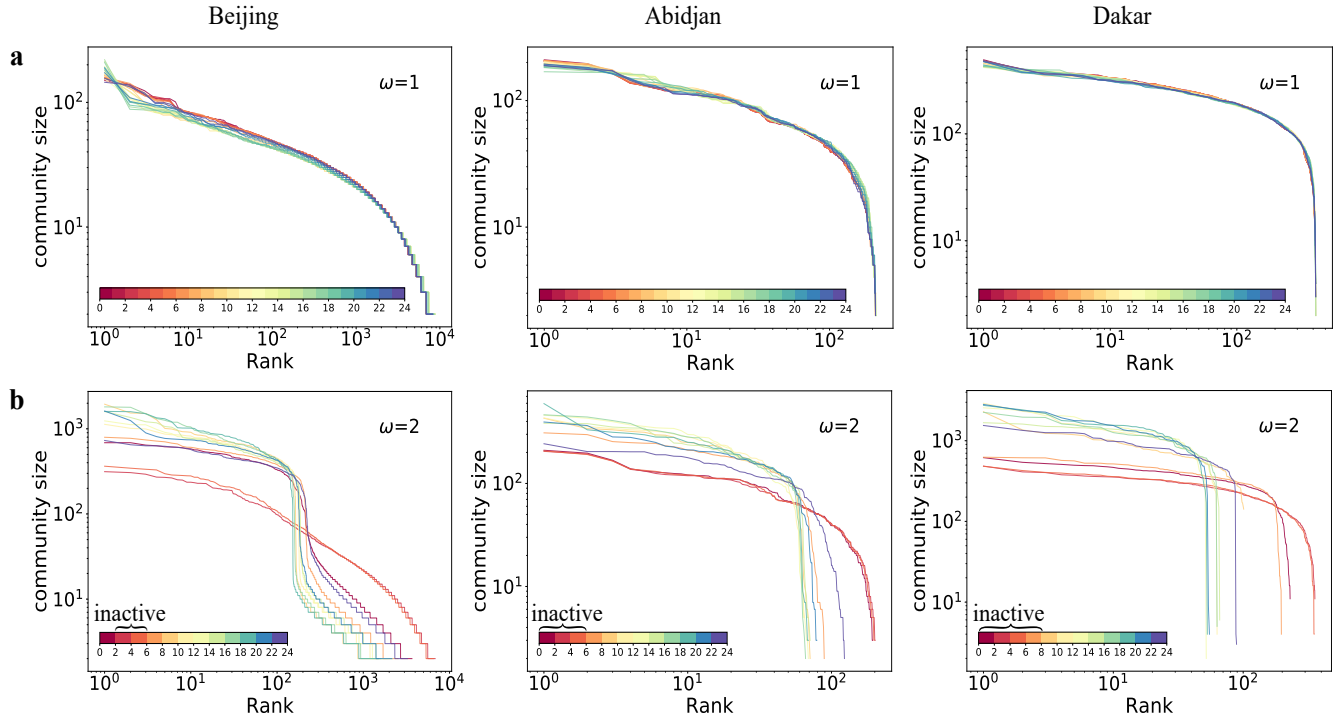


**Figure 2. The Zipfian rank-size distribution of communities with different time window sizes.** **a** When time window size  $\omega = 1$ , rank distributions of community size, which can be interpreted as hourly dynamic population, almost collapse together in all three diversified cities. Given the fact that people are almost constantly moving in cities, the stability of such distributions on population concentration is non-trivial. The scaling exponent of Beijing, Abidjan, and Dakar are 0.23, 0.17, and 0.09, respectively (see Supplementary Fig. 2 for more details). **b** When  $\omega = 2$ , a switching between active and inactive states is observed across cities, which is depicted by two distinguished distributions. This can be easily identified via visual inspections, and more quantitative evaluation can be found in Methods and Supplementary Fig. 6. In the active state, the city concentrates in fewer larger communities, while in the sleeping state, it scatters in more smaller communities. In addition, when a city grows larger, it “sleeps” for a shorter time. The community structure is detected by the Louvain algorithm<sup>43</sup>. The color of the line corresponds to different time periods as indicated in the color bar. There are 24 lines in **a** that correspond to networks in each hour, and 12 lines in **b**, each of which aggregates two consecutive networks in **a**.

### The switching of interaction states at urban scale

When aggregating spatio-temporal networks of consecutive time windows (see Fig. 1c, Fig. 2b, and Supplementary Figs. 2-4), the mobility of individuals are implicitly incorporated and an intriguing collective behavior emerged (see comparisons between Fig. 2b and Fig. 2a). Though the rank distributions of hourly dynamic population are stable, cities manifest a switching behavior between “active” and “sleeping” states, which are depicted by two distinguished rank distributions of community size (see Fig. 2b and Methods for more details). In the active state, people in the whole city are concentrated in fewer larger communities, which indicate that stronger interactions are happening between people. While in the sleeping state, the city is scattered in more smaller communities (see Fig. 2b). Such discoveries are universal across cities and are stable over different time window sizes  $\omega$  (see Supplementary Figs. 2-4 and Supplementary Note 2 for more details). In addition, when a city grows larger (e.g., from Dakar to Abidjan to Beijing), the city sleeps for a shorter time. This is consistent with the observation that the pace of life is faster in larger cities<sup>5</sup>. For instance, Beijing sleeps from 2 am to 6 am, Abidjan from 0 am to 6 am, and Dakar from 0 am to 8 am. We find that the population is the most deciding factor compared to other geographical, climatic factors, daylight length, temperature, and so on (see Table 1). Although the average temperature of Beijing is much lower than the other two, it is still the most active city among them.

### The relation between spatio-temporal interaction segregation and residential segregation

In previous literature, due to limitation on data accessibility, it is almost impossible to comprehensively study interaction segregation, thus most work focus on residential segregation as a proxy<sup>23,24</sup>. Residential segregation assumes that the home location of individuals impacts interactions with specific groups of people<sup>25,46</sup>. Traditional studies use social experiments



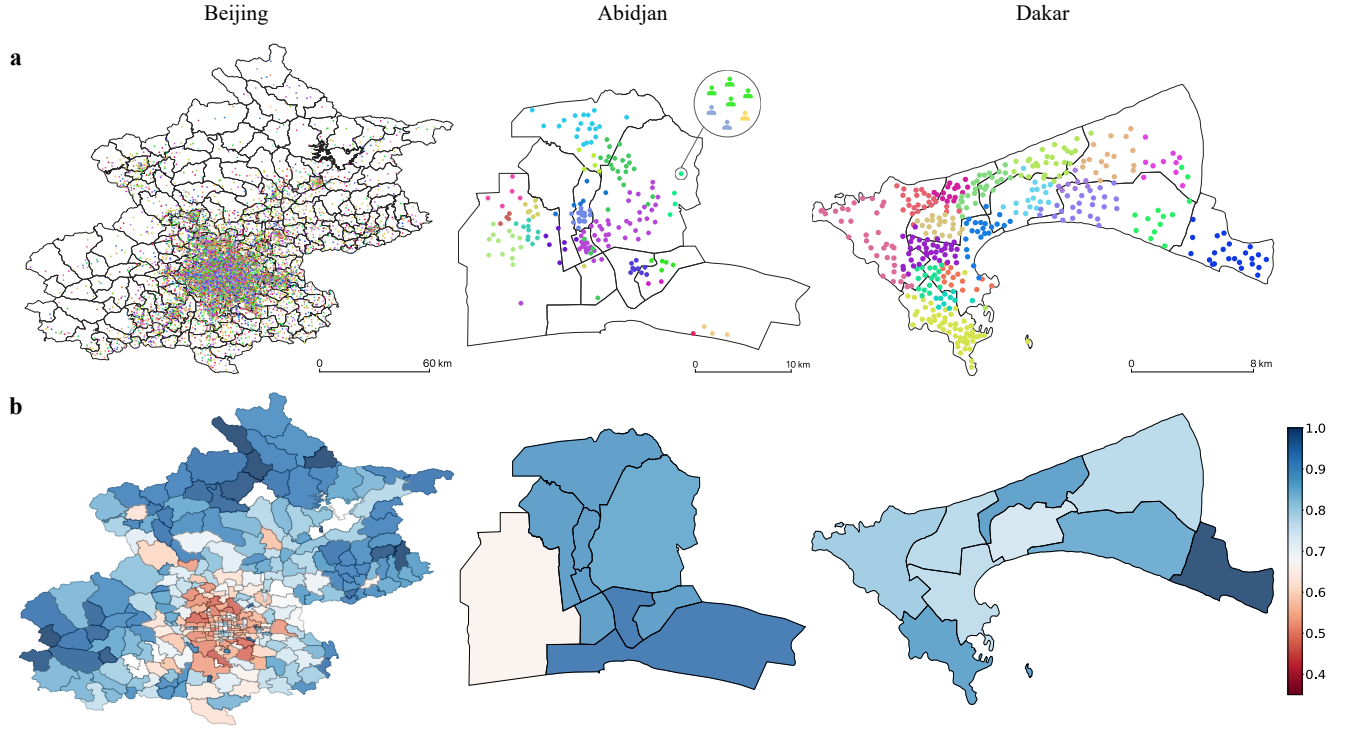


**Figure 3. Empirical results on the relation between spatio-temporal interaction segregation and residential segregation.** **a** The spatial distribution of interaction communities based on home locations of community members. The label of a location is determined by the majority rule (see the Inset in the middle). Different community labels are denoted by different colors. Each dot denotes a location. In smaller cities (see Abidjan and Dakar), residential segregation can well approximate the spatio-temporal interaction segregation, but not in larger cities (see Beijing). **b** The segregation index of each *Jiedao* in Beijing, *Commune* in Abidjan, and *Arrondissements* in Dakar. The average diameter of these administrative boundaries is around 7.96 km, 8.65 km, and 5.25 km, respectively.

or surveys to study residential segregation. With massive cellphone data, we are able to evaluate whether the residential segregation is representative of interaction segregation or not.

Here, we aggregate all spatio-temporal interaction networks in a day (i.e.,  $\omega = 24$ , see Supplementary Figs. 2-4), and the community segmentation is obtained by the Louvain algorithm<sup>43</sup>. Individuals in the same community have more overlaps in spatio-temporal trajectories and have a higher chance to interact with each other, however, interaction segregation might exist between individuals from different communities. Meanwhile, though the home location of individuals is not explicitly given by the cellphone data, it can be estimated by assuming that the residence is the location where the user has the highest appearance frequency between 10 pm and next 8 am<sup>36,37,40,41,47</sup>. By assigning the majority community label of residents to the location (see inset in the middle of Fig. 3a), we can then visualize the spatial distribution of interaction communities.

In smaller cities, communities generally locate within administrative boundaries. This indicates that individuals within the same spatio-temporal interaction community live spatially close, and residential segregation can be a good proxy of interaction segregation in smaller cities. However, in Beijing, there is no obvious correlation between them, as people who live in the same place can belong to different interaction communities (see Fig. 3a). This indicates that interactions in Beijing are more spatially mixed, which might be induced by various factors, including income level, transportation efficiency, mobility<sup>46</sup>. In bigger cities, residential proximity is not a good proxy of interaction patterns at urban scale.

Based on the fraction of different communities, we can further quantify the segregation level of a larger region (e.g., *Jiedao* in Beijing or *Commune* in Abidjan), which is composed of smaller locations. By generalizing the approach in ref.<sup>46</sup>, we can quantify the segregation index  $s_i$  of region  $i$  as

$$s_i = \frac{|C|}{2|C| - 2} \sum_{c \in C} \left| f_i(c) - \frac{1}{|C|} \right|, \quad (1)$$

where  $C$  is the set of unique community labels in the whole city, and  $|C|$  equals to the number of unique community labels,  $f_i(c)$  is the fraction of community label  $c$  in region  $i$ . The segregation index  $s_i$  is ranged from 0 to 1. When  $s_i = 0$ , all unique

communities are equally presented in  $i$ ;  $s_i = 1$  corresponds to the case that only one type of community exists in the region. In Beijing, regions near the city center are of a higher diversity as indicated by a low segregation index, and a spatial gradient can be observed (see Beijing in Fig. 5d). Such a pattern is less clear in Abidjan and Dakar (see Fig. 3b) due to possible impacts from various factors, including urban geography, socioeconomic development level, and population heterogeneity.

### Temporal population-weighted-opportunity (TPWO) mobility model

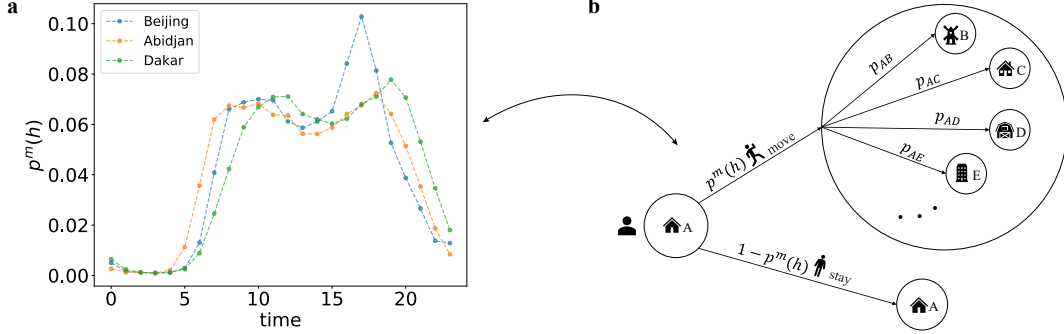


**Figure 4. The temporal population-weighted-opportunity (TPWO) model.** **a** The departure probability of individuals estimated from massive cellphone data in cities. **b** The schema of TPWO model that a user first decide whether to move based on the departure probability  $p^m(h)$  at time  $h$ , and if so, the probability of going to other locations (e.g.,  $p_{AB}$ ) is estimated according to Eq. 2.

To better understand possible factors influencing spatio-temporal interaction patterns in cities, we model mobility trajectory of individuals based on the well-known population-weighted opportunity (PWO) model<sup>48</sup>. Compared to other parameter-free mobility models<sup>49</sup>, PWO is more suitable for predictions at the intra-urban scale<sup>48</sup>. However, PWO neglects the temporal evolution of mobility and is only able to make static predictions for one step. When applied to model human mobility for multiple steps, it does not work well on reproducing observed spatio-temporal interaction patterns (see Supplementary Figs. 7-9). we propose a temporal population-weighted opportunity (TPWO) model by incorporating time-dependent departure probability  $p^m(h)$ , which is generally of two peaks (see Fig. 4). And  $p^m(h)$  is subject to the normalization condition that  $\sum_{h=1}^{24} p^m(h) = 1$ . At each time step, the probability of movement of an individual is first determined by  $p^m(h)$ . If so, the probability of moving from location  $i$  to  $j$  is estimated by

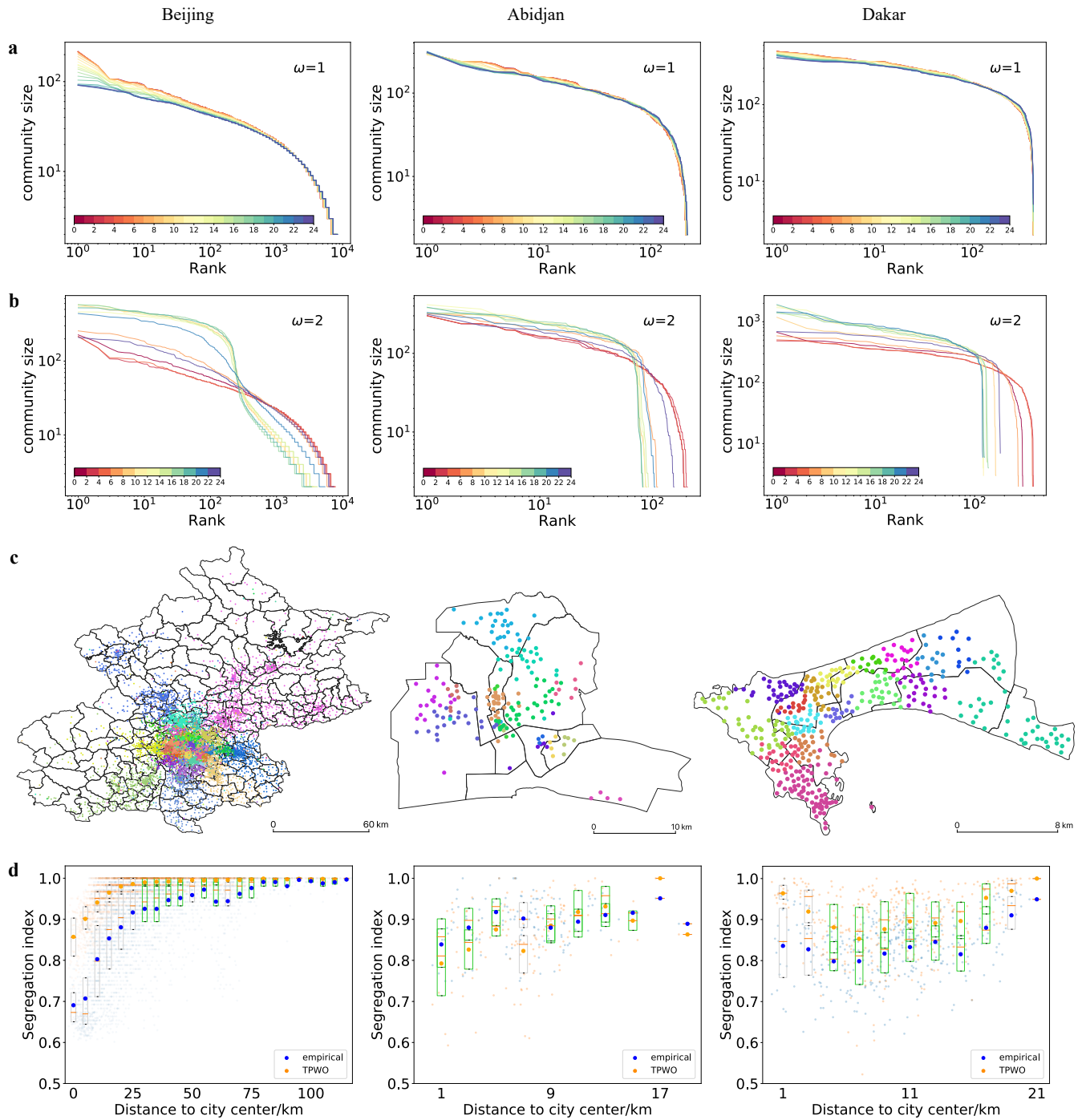
$$p_{ij} = \frac{T_{ij}}{T_i^{out}} = \frac{T_{ij}}{\sum_{j \neq i}^N T_{ij}}, \quad (2)$$

where  $T_{ij}$  is the volume of mobility flow from  $i$  to  $j$ , and  $T_i^{out} = \sum_{j \neq i}^N T_{ij}$  is the total outgoing flow from  $i$ .

$$T_{ij} = T_i \frac{m_j(1/S_{ji} - 1/M)}{\sum_{k \neq i}^N m_k(1/S_{ki} - 1/M)}, \quad (3)$$

where  $S_{ji}$  is the population in a circle with  $j$  as the center and the distance between  $i$  and  $j$  as the radius,  $m_j$  is the population of location  $j$ ,  $T_i^{out}$  is generally assumed to be proportional to  $m_j$ <sup>48,49</sup>,  $N$  is the total number of locations in the city, and  $M = \sum_j m_j$  is the total population of the city.

In our framework, we first initialize individuals to their home locations, and then simulate twenty-three steps of movements of each individual via the TPWO model to obtain the mobility trajectory. The size and initial spatial distribution of the simulated population are the same as users in cellphone data. From the obtained individual mobility trajectories, we construct the spatio-temporal interaction networks to study various interaction patterns at the urban scale. Empirical results show that the TPWO model can well reproduce stable distributions of hourly dynamic population (see Fig. 5a and Supplementary Figs. 7-9) and the switching behavior between two interaction states (see Fig. 5b and Supplementary Figs. 7-9). When the time window size  $\omega = 1$ , the rank distributions almost collapse together as observed in reality. As  $\omega$  increases, the switching behavior between two interaction modes emerges. As for the segregation patterns, smaller cities (Abidjan and Dakar) can be well reproduced in most regions (see Fig. 5c,d). In Beijing, we can reproduce the trend of the spatial gradient of segregation index but with relatively larger deviations near the central regions, which might be due to stronger mobility and population heterogeneity (see Fig. 5c,d).



In addition, it is worth noting that in mobility models, population is the most critical factor that measures the attraction of a location. The commonly used one is the residential population (RP), which is biased to working and business zones where the residential population (RP) is usually small but those regions are of high attractions. The active population (AP) that measures the number of individuals who have visited the location in a day<sup>3</sup> can be a much better proxy for the attraction of a location. We implement two versions of TPWO models, one is using RP, and the other is using AP of locations. TPWO model using AP has a better performance (see Supplementary Figs. 7-9 and Supplementary Note 3 for more details).

## Discussion

As rapid urbanization will continue in the next a few decades, gaining a deeper understanding of collective interaction patterns at the urban scale is crucial for inventing more livable, diversified, and prosperous future cities. In this context, our work has three useful findings. First, although people are almost constantly moving in the city, the rank distribution of the hourly dynamic population is not altered by the movements of individuals between locations. Human mobility can be regarded as perturbations to the system, the discovered stable rank distributions (see Fig. 2) imply that city can be regarded as a self-organized system<sup>50,51</sup>. And bigger cities are of a higher heterogeneity on dynamic population distribution, which is urban characteristic. Second, the observed switching behavior between active and sleeping states of cities is intriguing. In active states, individuals concentrate in fewer larger communities, which is similar to a reaction process that concentrates more energy and materials. While in sleeping states, the city is scattered into more smaller communities. In addition, when a city grows larger, it sleeps less. This is consistent with insights from urban scaling laws that the pace of life is faster in larger cities, and it would be interesting to investigate whether a city can be really sleepless if the population concentration continues. Third, residential segregation can be a good proxy of interaction segregation in smaller cities, but not in larger cities. To our best knowledge, such a relation is not well studied previously. And in Beijing, there is a clear spatial gradient of segregation index from the city center to the suburbs. The city center is shared by people from different groups and is an aggregator of diversity (see Supplementary Note 4 for more discussions). It is worth noting that now we are assuming local interactions between people who live closely still exist, if this is not the case in the future, then the spatial patterns of interaction communities in Beijing (see Fig. 3) might be the most segregated one: as people who live spatially close may not have strong interactions at all. Such a trend has already emerged in megacities, one may highly probably do not know the people who live above or below your apartment, or even just the next door. If the trend continues in the future, the city would separate people and local space meanwhile agglomerating the population.

All these findings contribute to gaining deeper understandings of emergent collective behaviors of cities and better managements of urban systems. For example, identifying close contacts of the infected patient based on community structures in spatio-temporal interaction networks, predicting the spreading paths, and intervening the spreading of COVID-19 in cities while preserving more interactions via dismantling the spatio-temporal interaction networks. The heterogeneous distribution of population and departure probability might be two key factors influencing the collective spatio-temporal interaction patterns of cities, which is revealed by our TPWO model. The deeper mechanics behind them are worth closer investigations in the future.

In addition, we also bridge the collective mobility model and spatio-temporal interaction patterns of individuals. The PWO model is a collective mobility model that is applied to predict the volume of flows between locations but not to predict individual mobility trajectories. By incorporating heterogeneous departure probability and making a partial homogeneous assumption, which assumes that individuals at a certain place will follow the ensemble mobility probability  $p_{ij}$  in Eq. 2 and the differences between individuals are only their home locations, the TPWO model can reasonably well reproduce collective spatio-temporal interaction patterns of cities. The TPWO model does not require detailed individual trajectory and other information, and only needs simple population-level inputs – departure probability and distribution of population, which can be easily obtained. Thus our framework provides a trade-off between privacy-preserving and studying spatio-temporal individual interaction patterns at the urban scale.

## References

1. Sim, A., Yaliraki, S. N., Barahona, M. & Stumpf, M. P. Great cities look small. *J. Royal Soc. Interface* **12**, 20150315 (2015).
2. West, G. *Scale: The universal laws of life, growth, and death in organisms, cities, and companies* (Penguin, 2018).
3. Li, R. *et al.* Simple spatial scaling rules behind complex cities. *Nat. Commun.* **8**, 1–7 (2017).
4. Bettencourt, L. M. The origins of scaling in cities. *Science* **340**, 1438–1441 (2013).
5. Bettencourt, L. M., Lobo, J., Helbing, D., Kühnert, C. & West, G. B. Growth, innovation, scaling, and the pace of life in cities. *Proc. Natl. Acad. Sci.* **104**, 7301–7306 (2007).

6. Alfeo, A. L., Cimino, M. G., Lepri, B., Pentland, A. S. & Vaglini, G. Assessing refugees' integration via spatio-temporal similarities of mobility and calling behaviors. *IEEE Transactions on Comput. Soc. Syst.* **6**, 726–738 (2019).
7. Logan, J. R. & Messner, S. F. Racial residential segregation and suburban violent crime. *Soc. Sci. Q.* **68**, 510 (1987).
8. Acevedo-Garcia, D. & Lochner, K. A. Residential segregation and health. *Neighborhoods Heal.* 265–87 (2003).
9. Tóth, G. *et al.* Inequality is rising where social network segregation interacts with urban topology. *Nat. Commun.* **12**, 1–9 (2021).
10. Jacobs, J. *The death and life of great American cities* (Vintage, 2016).
11. Song, C., Koren, T., Wang, P. & Barabási, A.-L. Modelling the scaling properties of human mobility. *Nat. Phys.* **6**, 818–823 (2010).
12. Schläpfer, M. *et al.* The universal visitation law of human mobility. *Nature* **593**, 522–527 (2021).
13. Alessandretti, L., Aslak, U. & Lehmann, S. The scales of human mobility. *Nature* **587**, 402–407 (2020).
14. Pan, W., Ghoshal, G., Krumme, C., Cebrian, M. & Pentland, A. Urban characteristics attributable to density-driven tie formation. *Nat. Commun.* **4**, 1–7 (2013).
15. Balcan, D. *et al.* Multiscale mobility networks and the spatial spreading of infectious diseases. *Proc. Natl. Acad. Sci.* **106**, 21484–21489 (2009).
16. Schläpfer, M. *et al.* The scaling of human interactions with city size. *J. Royal Soc. Interface* **11**, 20130789 (2014).
17. Li, R., Wang, W. & Di, Z. Effects of human dynamics on epidemic spreading in côte d'ivoire. *Phys. A: Stat. Mech. its Appl.* **467**, 30–40 (2017).
18. Deville, P. *et al.* Scaling identity connects human mobility and social interactions. *Proc. Natl. Acad. Sci.* **113**, 7047–7052 (2016).
19. Li, Q. *et al.* Early transmission dynamics in wuhan, china, of novel coronavirus–infected pneumonia. *New Engl. J. Medicine* (2020).
20. Oliver, N. *et al.* Mobile phone data for informing public health actions across the covid-19 pandemic life cycle. *Sci. Adv.* **6**, eabc0764 (2020).
21. Li, R., Richmond, P. & Roehner, B. M. Effect of population density on epidemics. *Phys. A: Stat. Mech. its Appl.* **510**, 713–724 (2018).
22. Batty, M. *The new science of cities* (MIT press, 2013).
23. Louf, R. & Barthélemy, M. Patterns of residential segregation. *PLoS One* **11**, e0157476 (2016).
24. Chodrow, P. S. Structure and information in spatial segregation. *Proc. Natl. Acad. Sci.* **114**, 11591–11596 (2017).
25. Wang, D. & Li, F. Daily activity space and exposure: A comparative study of hong kong's public and private housing residents' segregation in daily life. *Cities* **59**, 148–155 (2016).
26. Xu, Y., Belyi, A., Santi, P. & Ratti, C. Quantifying segregation in an integrated urban physical-social space. *J. Royal Soc. Interface* **16**, 20190536 (2019).
27. Helbing, D. Traffic and related self-driven many-particle systems. *Rev. Mod. Phys.* **73**, 1067 (2001).
28. de Dios Ortúzar, J. & Willumsen, L. G. *Modelling transport* (John wiley & sons, 2011).
29. Dong, L., Li, R., Zhang, J. & Di, Z. Population-weighted efficiency in transportation networks. *Sci. Reports* **6**, 1–10 (2016).
30. Li, R. *et al.* Gravity model in dockless bike-sharing systems within cities. *Phys. Rev. E* **103**, 012312 (2021).
31. Ruan, S. *et al.* Dynamic public resource allocation based on human mobility prediction. In *Proceedings of the ACM on Interactive, Mobile, Wearable and Ubiquitous Technologies*, vol. 4, 1–22 (ACM New York, NY, USA, 2020).
32. Lu, X., Bengtsson, L. & Holme, P. Predictability of population displacement after the 2010 haiti earthquake. *Proc. Natl. Acad. Sci.* **109**, 11576–11581 (2012).
33. Bagrow, J. P., Wang, D. & Barabasi, A.-L. Collective response of human populations to large-scale emergencies. *PLoS One* **6**, e17680 (2011).
34. Eagle, N. & Pentland, A. S. Reality mining: sensing complex social systems. *Pers. Ubiquitous Comput.* **10**, 255–268 (2006).



35. Blondel, V. D., Decuyper, A. & Krings, G. A survey of results on mobile phone datasets analysis. *EPJ Data Sci.* **4**, 10 (2015).
36. Xu, Y., Li, R., Jiang, S., Zhang, J. & González, M. C. Clearer skies in beijing—revealing the impacts of traffic on the modeling of air quality. In *Proceedings of the Transportation Research Board (TRB) 96th Annual Meeting*, vol. 17 (2017).
37. Xu, Y. *et al.* Unravel the landscape and pulses of cycling activities from a dockless bike-sharing system. *Comput. Environ. Urban Syst.* **75**, 184–203 (2019).
38. Blondel, V. D. *et al.* Data for development: the d4d challenge on mobile phone data. *ArXiv Prepr. ArXiv:1210.0137* (2012).
39. de Montjoye, Y.-A., Smoreda, Z., Trinquart, R., Ziemlicki, C. & Blondel, V. D. D4d-senegal: the second mobile phone data for development challenge. *ArXiv Prepr. ArXiv:1407.4885* (2014).
40. Alexander, L., Jiang, S., Murga, M. & González, M. C. Origin–destination trips by purpose and time of day inferred from mobile phone data. *Transp. Res. Part C: Emerg. Technol.* **58**, 240–250 (2015).
41. Çolak, S., Alexander, L. P., Alvim, B. G., Mehndiratta, S. R. & González, M. C. Analyzing cell phone location data for urban travel: current methods, limitations, and opportunities. *Transp. Res. Rec.* **2526**, 126–135 (2015).
42. Lockdown voices: Big-data glitches, yellow health-codes, and “spatial-temporal companions”. <https://chinadigitaltimes.net>. Accessed: 2021-12-06.
43. Blondel, V. D., Guillaume, J.-L., Lambiotte, R. & Lefebvre, E. Fast unfolding of communities in large networks. *J. Stat. Mech. Theory Exp.* **2008**, P10008 (2008).
44. Barbosa, H. *et al.* Human mobility: Models and applications. *Phys. Reports* **734**, 1–74 (2018).
45. Louail, T. *et al.* From mobile phone data to the spatial structure of cities. *Sci. Reports* **4**, 1–12 (2014).
46. Moro, E., Calacci, D., Dong, X. & Pentland, A. Mobility patterns are associated with experienced income segregation in large us cities. *Nat. Commun.* **12**, 1–10 (2021).
47. Jiang, S. *et al.* The timegeo modeling framework for urban mobility without travel surveys. *Proc. Natl. Acad. Sci.* **113**, E5370–E5378 (2016).
48. Yan, X.-Y., Zhao, C., Fan, Y., Di, Z. & Wang, W.-X. Universal predictability of mobility patterns in cities. *J. Royal Soc. Interface* **11**, 20140834 (2014).
49. Simini, F., González, M. C., Maritan, A. & Barabási, A.-L. A universal model for mobility and migration patterns. *Nature* **484**, 96–100 (2012).
50. Bak, P. *How nature works: the Science of self-organized criticality* (Springer Science & Business Media, 2013).
51. Christensen, K. & Moloney, N. R. *Complexity and criticality*, vol. 1 (World Scientific Publishing Company, 2005).
52. Ke, Q., Ferrara, E., Radicchi, F. & Flammini, A. Defining and identifying sleeping beauties in science. *Proc. Natl. Acad. Sci.* **112**, 7426–7431 (2015).
53. Doumbia, M. *et al.* Emissions from the road traffic of west african cities: Assessment of vehicle fleet and fuel consumption. *Energies* **11**, 2300 (2018).

## Methods

### Mathematical formalization of spatio-temporal interaction networks

Mathematically, a spatio-temporal interaction network  $\mathcal{G}(t)$  is defined based on the set of spatio-temporal co-occurrence events of individuals (i.e., edges in networks)

$$\mathcal{E}(t) = \{(u, v, t)\}, \quad (4)$$

where  $u, v \in V$  are individuals that appear at the same location at the same time window  $t$ , and  $V$  is the set of individuals. For higher accuracy, the resolution of the time window can be set quite small when the temporal resolution of the raw data is high. In this paper, for simplicity and without losing generality, we set the resolution of the time window as one hour. A specific spatio-temporal interaction network at time window  $t$  is then formulated as

$$\mathcal{G}(t) = \{\mathcal{V}, \mathcal{E}(t)\}. \quad (5)$$

$\mathcal{G}(t)$  is an undirected network. For simplicity, we assume that  $\mathcal{G}(t)$  is unweighted, where a non-zero  $A_{uv}(t)$  represents the spatio-temporal co-occurrence of  $u$  and  $v$  in the time windows  $t$ . The aggregation of co-occurrence events of consecutive time windows is formulated as

$$\mathcal{E}(t, t + \Delta t) = \{(u, v, t')\}, \quad (6)$$

where  $t' \in [t, t + \Delta t]$ . The aggregated spatio-temporal interaction network is defined as

$$\mathcal{G}(t, t + \Delta t) = \{\mathcal{V}, \mathcal{E}(t, t + \Delta t)\}. \quad (7)$$

The spatio-temporal co-occurrence events of individuals in  $\mathcal{G}(t, t + \Delta t)$  accumulate. For example, if  $(u, v, t = 1)$  and  $(u, v, t = 2)$ , then  $A_{uv}(1, 2) = 2$  in  $\mathcal{G}(1, 2)$  (i.e.,  $\Delta t = 1$ , which means the time windows size  $\omega = 2$ , see more details of the aggregation process in Fig. 1c). An aggregation of networks in more consecutive time windows (i.e.,  $\omega > 1$ ) generally increases overall connectivity of the graph, due to movements of individuals.

### Quantitative detection of switching between two interaction states

The switching between two interaction states can be easily noticed by visual inspections, and quantitatively, we find that the “turning point” of the curve<sup>52</sup> can be informative. The turning points of distributions in Fig. 2b should be the ones after which the curve decays faster. Generally, it is the farthest point from the straight line that connects the two ends of the curve (see Supplementary Fig. 6a). The rank value of turning points of distributions in working states is generally smaller than the ones of sleeping states, which gives a quantitative distinction between two states (see Supplementary Fig. 6b).

### Data availability

The cellphone data of Dakar and Abidjan is shared by organizers of Data for Development Challenges<sup>38,39</sup>, the one of Beijing is provided by a local telecommunication operator under a non-disclosure agreement. The shapefile of Abidjan at the commune resolution is from ref.<sup>53</sup>. Other additional data related to this paper are publicly available and may be requested from the authors.

### Acknowledgements

This work receives financial supports from the National Natural Science Foundation of China (Grant No. 61903020), Fundamental Research Funds for the Central Universities (Grant No. buctrc201825). We acknowledge organizers of Data for Development (D4D) Challenges for sharing cellphone data of Senegal and Côte d’Ivoire, and Dr. Madina Doumbia from University Péléforo Gon Coulibaly for providing the shapefile of Abidjan at the commune resolution.

### Author contributions statement

R.L. conceived and supervised the research, C.L., Y.Y., T.C., and F.S. analyzed data, C.L. constructed the mobility model, C.L., R.L., and B.C. analyzed and discussed the results. B.C., C.L., and R.L. wrote the manuscript. All authors reviewed the manuscript.

### Competing interests

The authors declare no competing interests.

### Additional information

Supplementary information is available for this paper at .